

Quantification of soil macroporosity and its relationship with soil properties

S.N. ASARE¹, R.P. RUDRA¹, W.T. DICKINSON¹ and A. FENSTER²

¹*School of Engineering, University of Guelph, Guelph, ON, Canada N1G 2W1; and* ²*Imaging Research Laboratories, The John P. Robarts Research Institute, 100 Perth Drive, London, ON, Canada N6A 5K8. Received 23 July 1998; accepted 16 February 1999.*

Asare, S.N., Rudra, R.P., Dickinson, W.T. and Fenster, A. 1999. **Quantification of soil macroporosity and its relationship with soil properties.** *Can. Agric. Eng.* 40:023-034. Image analysis was used to estimate macroporosity (pores ≥ 0.54 mm in diameter) of undisturbed soil columns obtained from a field under no-till for 5 years. A high resolution x-ray Image Intensifier (XRII)-based CT scanner was used to investigate soil macroporosity at different depths in the soil column. Total macroporosity in the A and B horizons averaged 3.70 and 1.94%, respectively, and was consistently lower in the B-horizon. The relative contributions of macroporosity to the total porosity in the A and B horizons were 7.76 and 4.92%, respectively. There was a statistically significant decreasing trend of macroporosity through the combined A and B horizon depth (0 - 400 mm) and in the A horizon (depth 0 - 200 mm), but not in the B-horizon (depth 200 - 400 mm). Saturated hydraulic conductivity correlated significantly with the total macroporosity of the A and the B horizons, within the A horizon, bulk density also significantly correlating with total macroporosity. **Keywords:** bulk density, computer tomography, image analysis, macroporosity, hydraulic conductivity, no-till.

Des techniques d'analyse d'images furent utilisées pour évaluer la macroporosit  (pores ≥ 0.54 mm de diam tre) de colonnes de sol non d rang  provenant d'un champ o  il n'y avait pas eu de travail du sol depuis 5 ans. On a utilis  un tomodensitom tre assist  par ordinateur (CT scanner) op rant avec un intensificateur d'image   rayons-X (XRII) pour examiner la macroporosit  du sol   diff rentes profondeurs dans la colonne de sol. La macroporosit  totale dans les horizons A et B  tait en moyenne de 3.70 et 1.94%, respectivement, et  tait r guli rement plus faible dans l'horizon B. La contribution relative de la macroporosit    la porosit  totale  tait, dans les horizons A et B, de 7.76 et 4.92% respectivement. On a observ  une tendance   la baisse statistiquement significative de la macroporosit    travers les horizons A et B combin s (0 - 400 mm), et dans l'horizon A seul (0 - 200 mm), mais pas dans l'horizon B (profondeur 200 - 400 mm). Il y avait une corr lation significative entre la conductivit  hydraulique et la macroporosit  totale des horizons A et B. Pour l'horizon A, on a aussi  tabli une corr lation significative entre la densit  apparente et la macroporosit  totale. **Mots-cl s:** densit  apparente, tomodensitom trie assist e par ordinateur, analyse d'images, macroporosit , conductivit  hydraulique, travail r duit du sol.

INTRODUCTION

The influence of soil macropores on transport of water, agrochemicals, and bacteria through soil profiles and subsequently into subsurface water systems is now well accepted (Steenhuis et al. 1990; Gish et al. 1991; McMahon and Thomas 1974). Soil macropores move significant volumes of free surface water deeper into the soil profile and at higher velocities than would be predicted by the Darcian approach (Quisenbury and Phillips 1978; Gardner 1962). In view of the observed transport

capabilities of soil macropores, their presence in agricultural fields is of particular concern, especially in fields where no-tillage management practices are predominant. This concern is related to: (i) greater utilization of agro-chemicals and fertilizers in no-till systems, with these additives left on or near the soil surface to control weeds, insects and disease problems, and to supplement crop nutrients (Shipitalo and Protz 1987; Steenhuis et al. 1990); (ii) increased amounts of soluble chemicals and nutrients in surface and subsurface flow that can readily enter soil macropores (Gish et al. 1991; Steenhuis et al. 1990); (iii) lack of periodic disruption of macropore systems in no-till plots; and (iv) enhancement of activities of soil organisms such as earthworms, termites, and gophers because of crop residues left on soil surfaces under prolonged no-till management (Li and Ghodrati 1994; Shipitalo and Protz 1987). Studies have also revealed that substituting no-till for conventional tillage greatly reduces runoff and subsequently increases the amount of water available for percolation (Edwards et al. 1988; Steenhuis et al. 1990).

Numerous direct approaches have been used to estimate physical characteristics of macropores, including their size, distribution, and orientation within the soil profile. Macropore dimensions have been directly measured (Ehlers 1975; Bouma 1981). Two commonly-used direct approaches involve the use of dye and image analysis techniques. In the dye technique, direct measurements of macropore dimensions are made for each layer along the soil profile after application of an adsorbing dye and a tracer on the soil surface to mark pathways followed by dissection of the soil column (Steenhuis et al. 1990; Omoti and Wild 1979). In the image analysis technique, hardeners or latex compounds are used to impregnate soil pores and the porosity is scanned with image analysis to trace the path of soil macropores (Moran et al. 1988; Bullock and Thomasson 1979). Major drawbacks of these direct approaches are that the methods do not give an indication of continuity of macropores and column samples cannot be used for further experimental tests and investigations because each soil column has to be dissected (Omoti and Wild 1979; Smettem and Collis-George 1985).

A method which has the potential to characterize macropore continuity including both channelling and non-channelling components, involves the use of an X-ray Computer Tomography (CT) Scanner (Anderson et al. 1988, 1990; Warner and Nieber 1991; Peyton et al. 1992). This CT scanner has potential for combining investigations of macropore structure

and continuity with flow investigations on the same soil column (Warner et al. 1989).

Many encouraging attempts have been made to apply the CT scanning techniques in soil science studies, particularly for investigating soil macropores (Anderson et al. 1988; Warner et al. 1989; Warner and Nieber 1991; Peyton et al. 1992). The CT technique has also been used to investigate soil water content and solute transport in soil columns (Anderson et al. 1988), as well as in soil compaction and bulk density studies (Petrovic et al. 1982). A number of studies have been conducted to evaluate soil macropores using a CT scanner; however, the CT technique has not been applied to characterize soil macropores in undisturbed no-till soils to quantitatively relate soil macropores at different depths with soil properties.

Most soil macropore studies involving the use of a CT scanner have used either packed soil samples (Anderson et al. 1988; Joschko et al. 1991) or undisturbed soil samples obtained from fields under various forms of management practice (Moran et al. 1988; Peyton et al. 1992, 1994; Warner and Nieber 1991; Anderson et al. 1990). Peyton et al. (1992, 1994) used the x-ray CT scanner technique to compare differences in macropore characteristics in undisturbed soil cores taken from a natural forest and a field with perennial grasses. Anderson et al. (1990) evaluated constructed and natural soil macropores in the A-horizon of soil from a conventional tillage site and from a natural forest site. Warner and Nieber (1991) investigated macropore distribution in tilled and grass-covered core samples using the CT scanner technique.

Fluid transport studies involving no-till soils and soil macropores have focused mainly on the movement of water and solutes in the presence of macropores (Shipitalo et al. 1990; Singh and Kanwar 1991; Andreini and Steenhuis 1990). Singh and Kanwar (1991) conducted miscible displacement experiments using chloride in large undisturbed saturated soil columns from no-till and conventional tillage plots to compare preferential solute movement through macropores. Their results indicated that the degree of preferential flow was greater in no-till than in conventional tillage columns. Shipitalo et al. (1990) investigated the initial macropore transport of surface-applied chemicals in blocks of soil obtained from a long-term, no-till corn field. Other soil macropore studies involving soil macropore characterization and/or solute transport have been based on packed soil samples (Li and Ghodrati 1994) and monoliths taken from fields other than no-till conditions (Quisenberry et al. 1994; Wildenschild et al. 1994).

Studies to date have contributed to our present knowledge of macropores and their influence on soil water flow and solute transport in soil. What is missing is an in-depth investigative study of soil macropores in agricultural fields under continuous no-tillage practice. The objectives of this study have been to apply a high-resolution laboratory volume CT scanner, designed to provide high spatial resolution in all three dimensions, to undisturbed soil column samples from a no-till plot in an attempt to quantitatively evaluate differences and trends in macroporosity at different depths in the A and B-horizons. A complementary objective was to check the merits of CT-scanning by correlating CT-scanned macroporosity with conventionally-measured soil physical properties.

MATERIALS and METHODS

Soil preparation

The soil used in this study was obtained from the Agricultural and Agri-Food Canada Research Field at Belmont, ON. This site has been under no-till conditions since 1989, with a crop rotation of corn and soybeans. The soil belongs to the Tavistock series (Gray Brown Luvisol), mostly developed on loam and silt loam sediment over clay (Agriculture Canada 1990). The predominantly silt loam A and B horizons have average depths of 200 mm each.

Eight undisturbed soil blocks measuring 120 mm x 120 mm x 400 mm were obtained from a random sampling of the research field using the excavation method described by Murphy et al. (1981). The first part of this method involved rough excavation to isolate soil pedestals measuring 200 mm x 200 mm x 400 mm using a shovel. With the support of specially designed boards placed at the sides of each pedestal, each side was carefully trimmed with a trowel and knife until a final size of 120 mm x 120 mm x 400 mm was obtained. Each block was then placed between Plexiglas sheets and tightly taped together to hold the soil firmly. Subsequently each block was cut off at the bottom and sealed firmly with tape. Also, during the excavation, three sets of soil samples were collected from the A and B-horizons. These included grab samples and two sets of core samples of diameter 50 mm and lengths 25 and 50 mm, respectively. The blocks were taken to the laboratory and stored in a controlled climatic chamber to reduce biological activities in the soil.

The soil blocks were removed from the Plexiglas container and the corners were carefully and gently scraped with a sharp knife, until the shape of each block approximated a circular column 90 mm in diameter. Each 400 mm column was divided into two columns, each 200 mm long, approximately representing the A and B horizons. These columns are referred to later as samples S1A, S1B, S2A, S2B,.....,S8A and S8B, where A and B indicate the A and B horizons of each respective sample (the A-horizon component of sample S3 was damaged in the course of the preparation).

The columns were wrapped in plastic and sealed with tape to eliminate evaporation. Each soil column was placed inside a specially designed Plexiglas tube (diameter 100 mm and height 250 mm) with top and bottom covers to fit onto the specimen stage of the CT Scanner. Two cylindrical tubes, each with an internal diameter of 5 mm and a length of 200 mm, were filled with air and water, respectively. These tubes were sealed at both ends, placed alongside the soil columns inside the CT sample tube, and used as standards to assist in the detection and interpretation of the results of the images of the soil columns obtained from the CT scanner. The remaining space around the soil column tube was filled with fine commercial sand to stabilize the soil column in the CT sample tube (Fig. 1).

The other soil samples collected during excavation were analyzed for soil texture and organic matter using standard methods (McKeague 1978). Soil water content and bulk density were determined from a mass-volume relationship after oven-drying a known volume and mass of the core samples at 105 °C for 24 hours. Total porosity (f) was estimated from bulk density and an assumed particle density value of 2650 kg/m³.

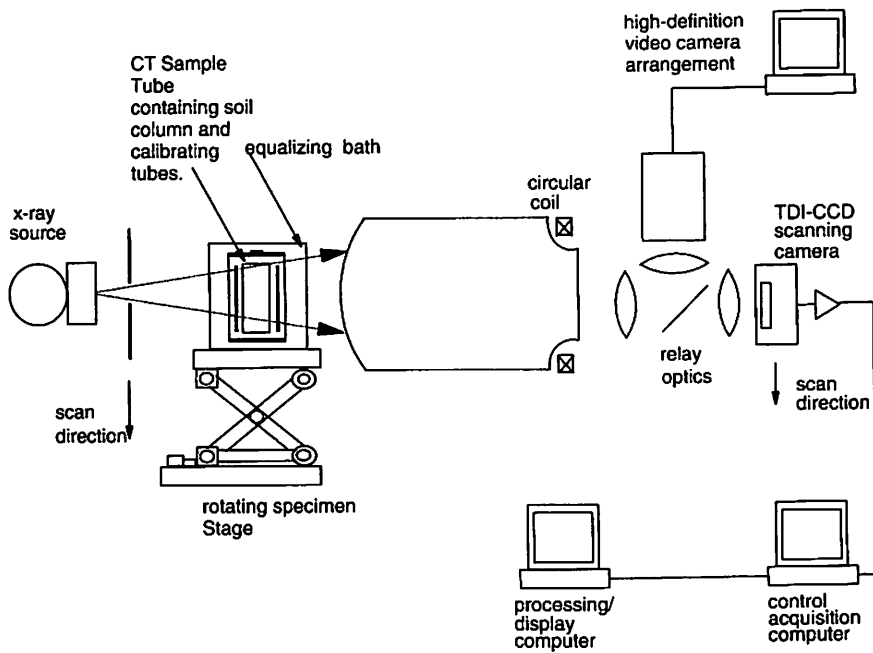


Fig. 1. Schematic diagram of the volume CT scanner.

The use of CT techniques in soil macropore studies have been hampered by limited access to suitable CT machines dedicated for the most part to hospital use. It is therefore important to define, if possible, relationships between soil macroporosity and easily measurable soil physical and hydraulic properties in order to maximize benefits derived from expensive CT-macroporosity. In this study, an initial screening was done to investigate a subset of measured soil properties that have or could predict the soil macroporosity. Principal component analysis (PCA) was used to select a subset of variables and a multiple regression analysis was used to fit the coefficient for the subset of variables selected. The soil properties considered in the PCA were: percentage sand, silt, and clay, water content, bulk density, and saturated hydraulic conductivity.

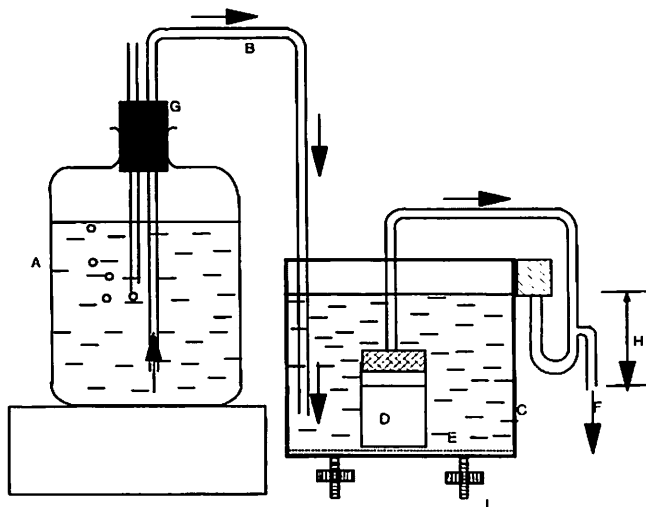


Fig. 2. Constant head permeameter for determining the saturated hydraulic conductivity of soil cores in the laboratory.

The 50 mm length core samples collected at each horizon during the excavation of the soil blocks were used to determine the saturated hydraulic conductivity, K_s , using a steady upward flow constant head permeameter setup shown in Fig. 2. This unit was designed in the laboratory to hold multiple core samples of 10 at a time. The soil core samples were placed in the trough and connected u-tubes were seated outside the trough, with measuring cylinders to collect outflow of water from each core sample. The volume of water collected for a given time period was used to calculate K_s using:

$$K_s = \frac{Vl}{A \Delta H \Delta t} \quad (1)$$

where,

K_s = saturated hydraulic conductivity (m/s),

V = volume of water passing through sample in a given time (m^3),

l = length of soil core sample (m),

A = cross-sectional area of the core sample (m^2),

ΔH = hydraulic head difference across core sample (m), and

Δt = time period for each outflow measurement (s).

X-Ray image intensifier (XRII)-based volume CT scanner

The XRII-based volume CT scanner (Imaging Research Laboratories, The John P. Roberts Research Institute, University of Western Ontario, London, ON), with a high resolution in all three dimensions, was used in this study (Fig. 1). The system uses an X-ray image intensifier coupled to a low-noise time-delay integration (TDI) area charge-couple device (CCD) to obtain projections from different angles around a rotating sample. In the volume acquisition mode used to scan the soil columns, the detector was operated in synchrony with a collimated fan beam of X-rays to obtain a two-dimensional projection image at each angular position around the object. The volume acquired by the system in this manner allowed the reconstruction of an image with high resolution in all three spatial dimensions. This procedure helped to reduce the effects of partial volume artifacts (Holdsworth et al. 1993).

The factors associated with the CT scanner, including the X-ray energy, focal points, object distances, rotation angles, stage height, and most of the internal conditions, were controlled by the control acquisition computer. The X-ray intensity was set at 93 kVp

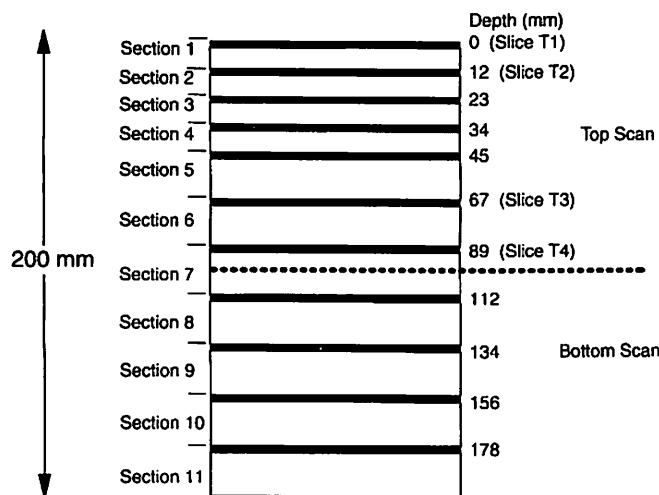


Fig. 3. Schematic diagram describing the division of image data into sections for analysis after scanning. Slices T1, T2, T3, T4 were selected for the calibration of the cut-off gray value for the top scan of sample S1A. (Diagram not to scale.)

and 30 mA with 6.5 mm added filtration and the scanning was made at a field of view (FOV) of 115 mm. Each column in the CT sample tube was then mounted on the rotating specimen stage inside a rectangular equalization bath. Each column was scanned in two sections, the top section and the bottom section, to accommodate the maximum FOV of the CT scanner. Markers were placed on the sides of the tube for easy identification of the separate top and bottom scans for each column.

The resolution of the CT scanner refers to either the smallest spatial dimension that is the voxel size or the smallest changes in attenuation properties that can be detected using the scanner. The size of each voxel in the image depends on two factors, the geometrical magnification and the field of view. Boundary effects occur when the density at the boundary of a heterogeneous material falls in the middle of a pixel or voxel in a CT scan image rather than on the edge. The attenuation value calculated by the scanner will therefore be a composite or average of the different materials lying within the pixel edges, which makes the determination of the true value more difficult for heterogeneous materials like soil. This compounds the difficulty in characterizing soil macropores that may appear as small objects embedded in a much larger mass. In relation to macropores, it is usually appropriate to define pore size such that at least one pixel size should fall entirely upon the pore so as to produce the true attenuation of the pore (Warner et al. 1989).

Based on the spatial resolution determined by the CT scanner as a result of the field of view selected for the scanning of the soil columns (115 mm), a pixel value of 0.24 x 0.24 mm, and a corresponding z component of 0.27 mm was estimated from a calibrated graph. The practical effective pore diameter which was considered in estimating the macroporosity was 0.54 mm, i.e. the diameter of the area covered by twice the pixel size. This diameter was selected to constitute the pore size

which the volume CT scanner could clearly identify and the macroporosity of the soil column was based on this pore diameter.

Data collection and image analysis

The scanning procedure generated a three-dimensional gray-level image of the soil column after reconstruction. Each volume element (voxel) was represented by a single gray value (0 - 255) in these data. Each gray value represented the intensity of the X-ray signal detected for that voxel (zero for most dense or black and 255 for least dense or white medium). Each voxel measured 0.24 mm in the x-direction, 0.24 mm in the y-direction and 0.27 mm in the z-direction (depth of a single slice or tomograph). The image data for each soil column was subdivided into sections of thickness 12 mm and 22 mm (Fig. 3), consisting of approximately 44 and 81 slices, respectively. For each soil column, an average of eleven slices representing the first slice for each section of the soil column (Fig. 3), with thickness corresponding to the thickness of each voxel (0.27 mm), were taken for the image analysis. These represent slices at depths of 0, 12, 23, 34, 45, 67, 89, 112, 134, 156, 178, and 185 mm of each soil column. Each slice provided a cross-section of the three-dimensional image for the content of the CT sample tube, namely: the soil column, the air tube, the water tube, and the sand used to fill the sides of the CT sample tube.

For every column, the calibration of each independent (top and bottom) scan involved the selection of four slices (T1 and T2 from the two upper sections and T3 and T4 from the two lower sections) from the top scan as shown for S1A in Fig. 3. The image data for each slice was displayed using the IMAGEWORKS module of the EASI/PACE program (PCI Software 1994). Regions of interest consisting of air and water from the cylindrical tubes and a portion of the soil column alone (excluding the sand) were demarcated for the analysis using the TRAIN function. The HIS function of the EASI/PACE program was used to estimate the means, medians, and standard deviations of the gray value signals representing each of the voxels (voxel value) in the selected regions of the image.

Based on the mean voxel values and the standard deviations obtained for the air and the water regions of each selected slice in an independent scan, a cut-off value was estimated to represent the voxel gray value representing pores in that resulting image data from the scan. The lowest average gray value corresponding to water was estimated to represent the cut-off value for pores and soil matrix. The value for water was used because the average gray value for water was lower than those for air and higher than that of soil. To account for all the pores containing water, the lowest gray value representing water in that particular scan had to be used as the cut-off point where all gray values higher than that value were considered as pores and gray values less than that as soil matrix.

Table I presents the cut-off gray values for sample S1A top scan (171) and S1A bottom scan (127) and how they were estimated. The scanning procedure is clarified by reference to these sample data. The soil column S1A was scanned in two parts, i.e., the top and bottom scans (Fig. 3). T1, T2, T3, and T4 indicate the four slices selected to determine the cut-off gray

Table I. Data from column S1A describing the procedure used to determine the cut-off gray value for the image from the CT scan (cut-off gray values for pores are in parenthesis and mean and standard deviation values used to estimate the value are bold-faced).

	Top-scan S1A (171)				Bottom-scan S1A (127)			
	T1*	T2	T3	T4	T1	T2	T3	T4
Air								
Number of voxels	89	55	79	82	107	89	95	102
Mean grey value	183	188	185	187	131	131	133	134
Median grey value	183	189	185	186	131	131	132	133
Std. Deviation	5.6	3.5	5.8	4.5	1.9	1.8	2.1	3.1
Water								
Number of voxels	68	80	104	95	142	145	140	135
Mean grey value	174	179	174	176	129	128	129	129
Median grey value	174	180	175	178	129	128	128	129
Std. Deviation	1.3	2.1	2.6	1.5	0.6	0.7	1.1	1.3
Soil								
Number of voxels	3914	2240	3288	3500	2407	2458	2145	2587
Mean grey value	147	153	153	159	121	122	121	120
Median grey value	147	152	152	157	121	121	122	122
Std deviation	2.6	4.8	3.6	5.2	2.7	1.8	1.7	1.5

*T1, T2, T3 and T4 are the slices that were selected from each section of the column

value for the top scan. The number of voxels (n), mean, median, and standard deviation of voxel gray values of the region of interest selected from each slice are estimated and listed under each column. The mean gray value for water lies between that of air and soil. Hence, to establish a gray value cut-off point to represent pores in the soil column, the lowest gray value representing that of water in the four slices was estimated (lowest among the means less one standard deviation for the four slices). The value of 171 was estimated for the S1A top-scan based on slice T3, which had a mean gray value of 174 with a standard deviation of 2.6. This lowest gray value was selected to represent pores in the soil column for the top-scan of S1A. These values were different for each scan, prompting the need for the air and water tubes beside the soil columns for all the samples.

After the cut-off gray value for each independent scan was established, a region of interest representing the actual soil column was selected and the HIS function of the EASI/PACE program was used to estimate the cumulative frequency of the total number of voxel values within each selected tomograph. The total percentage of pores at each given depth with effective diameters greater than 0.54 mm was used to represent the macroporosity at that depth.

RESULTS and DISCUSSION

Soil physical properties

A number of observations about the test soils was made in the course of the excavation. Among these were the visible differences in coloration between the A and the B horizons. The A-horizon was a very dark grayish brown and the B-horizon was a dark yellowish brown with blocky subangular structure at its lower depth. There were visible macropores, mostly cylindrical, of different sizes and orientations. Most of the macropores were likely created by earthworms; some worms were still occupying parts of the channels. No observations were made of structural cracks in the A-horizon, but the blocky structure lower down in the B-horizon showed a few structural cracks and cleavages.

Table II presents the results of selected soil properties that were investigated to help understand the estimated macroporosity at the different depths and to compare spatial differences in the A and B horizons. For each property the data from each horizon were considered as independent groups and their means were tested for differences using the two-sample t-test (Hirsch et al. 1992; SYSTAT for Windows 1992).

The data from Table II show that the mean values of bulk density (1376 and 1604 kg/m³ for A and B horizons, respectively), total porosity (48.1 and 39.5%, respectively), and organic matter content (3.7 and 1.3%, respectively) were found to be significantly different ($P < 0.05$). The mean values of the three textural classes of sand, silt and clay, in addition to the water content at the time of sampling, were found not to be significantly different between the A and B horizons.

In terms of the heterogeneity of the two horizons, the A-horizon data indicated a greater variation in the bulk density, with a greater standard deviation of 63.2 kg/m³ and a coefficient of variation of 4.6%, in comparison to the B-horizon with a standard deviation of 38.1 kg/m³ and a coefficient of variation of 2.4%. These results indicate greater heterogeneity in the A-horizon than in the B-horizon. The higher bulk density in the B-horizon could be attributed to reduced disturbance of the B-horizon, since the field had been under no-tillage for more than five years before the samples were taken and had been cultivated mostly with shallow-rooted crops like corn. Another factor that may have contributed to the higher bulk density in the B-horizon is the lower organic matter content, as well as greater compaction of the soil particles.

Table II. Selected soil properties of a no-till silt loam soil from Belmont, ON including organic matter (OM), degree of saturation (s), total porosity (f), volumetric water content (θ_v), bulk density (β_b), and saturated hydraulic conductivity (K_s). Each is the average of three sub-samples (taken in September, 1993).

Sample	Sand	Silt	Clay	OM	s	f	θ_v	β_b	K_s
	----- (%) -----				----- (m ³ /m ³) -----			(kg/m ³)	(10 ⁻⁵ m/s)
A-horizon (0 -200 mm)									
S1A	25.0	53.5	21.6	3.6	0.764	0.445	0.335	1470	0.52
S2A	28.3	53.3	18.4	4.1	0.682	0.513	0.348	1290	1.97
S3A	27.3	55.4	17.5	3.7	0.693	0.476	0.334	1390	3.00
S4A	29.2	54.9	16.0	3.4	0.783	0.460	0.361	1430	1.44
S5A	30.0	53.3	16.3	3.5	0.713	0.491	0.351	1350	1.14
S6A	26.5	54.2	19.3	3.7	0.754	0.464	0.346	1420	1.83
S7A	29.2	52.6	18.2	3.8	0.688	0.509	0.351	1300	2.03
S8A	26.0	54.7	19.3	3.9	0.719	0.487	0.350	1360	1.06
Mean	27.7 ^{NS}	54.0 ^{NS}	18.3 ^{NS}	3.7*	0.725*	0.481*	0.35 ^{NS}	1376*	1.70 ^{NS}
S.D.	1.66	0.90	1.69	0.21	0.036	0.024	0.007	63.2	0.73
CV (%)	6.0	1.7	9.2	5.6	4.9	5.0	1.9	4.60	42.5
B-Horizon (200-400 mm)									
S1B	13.2	51.2	35.7	1.5	95.0	0.400	0.384	1600	1.61
S2B	24.8	45.7	29.6	1.2	81.7	0.404	0.325	1580	1.82
S3B	28.0	52.6	19.5	0.8	92.4	0.377	0.345	1650	1.46
S4B	29.3	58.7	12.1	1.0	82.3	0.389	0.321	1620	1.30
S5B	27.6	54.7	17.8	1.9	75.7	0.423	0.323	1530	3.27
S6B	21.2	55.8	23.0	1.5	84.8	0.381	0.331	1620	4.50
S7B	26.5	53.0	23.0	1.5	86.6	0.382	0.330	1640	2.07
S8B	26.8	57.6	15.6	1.1	85.0	0.400	0.342	1590	2.56
Mean	24.7	53.7	22.0	1.3	85.4	0.395	0.337	1600	2.32
S.D.	4.90	3.83	7.16	0.33	5.70	0.014	0.019	34.0	1.02
CV (%)	19.9	7.1	32.5	25.1	6.7	3.5	5.7	2.2	43.9

* mean of property is significantly different ($P < 0.05$) between the A and B horizons, using independent sample t-Test for means grouped by horizons.

^{NS} mean between A and B horizon not significantly different.

Total macroporosity

All single slices obtained from the top of each section of each soil column (at different depths) were analyzed for macroporosity. In all cases, voxels with gray values higher than

the cut-off value were considered to be pores, whereas those with lower values were considered to be soil micropores. The value of macroporosity obtained was used as a representative macroporosity for the section or the depth of the column that the section represented. The mean of the values at the different depths was used to represent the total macroporosity for each soil column sample. Data presented in Tables III and IV show the change in macroporosity with depth for each soil column for the A and B-horizons, respectively.

The A-horizon had an average total macroporosity of 3.70%, with values ranging from a low of 2.59% in sample S8 to a high of 4.49% in sample S1. On the average, macroporosity in the A-horizon decreased from a value of 5.58% at the surface to 2.45% at a depth of 189 mm, with a coefficient of variation of 37.8%. Figure 4 presents data on the average macroporosity at the different depths for the A and B horizons. The B-horizon had a mean macroporosity of 1.94%, a value significantly lower than that for the A-horizon ($P < 0.05$). Wildenschild et al. (1994) estimated variation of macroporosity based on a much larger pore diameter (between 2.2 and 4.7 mm), and obtained a lower range of 1.2 and 2.7% along the depth of 0 - 500 mm. Although the soils and management practices are different, the magnitude of the macroporosities are comparable.

The data for the change in macroporosity with depth for the B-horizon samples (Table IV) show that the total macroporosity of the B-horizon was consistently lower than that in the corresponding A-horizon (Fig. 5). The only exception was sample S6 at the depth of 12 mm from the top of

Table III. Soil macroporosity distribution with depth in the A-horizon of a no-till silt loam soil from Belmont, ON estimated from CT scanning.

Depth (mm)	Macroporosity (%) - A-Horizon							
	S1*	S2*	S4*	S5*	S6 ^{NS}	S7 ^{NS}	S8 ^{NS}	Mean ^{&}
0	9.78	4.52	7.90	5.92	4.73	3.47	2.74	5.58a
12	5.93	7.54	5.80	5.49	6.55	2.26	3.63	5.31b
23	9.59	3.87	7.47	3.86	7.30	4.53	3.66	5.75c
34	6.80	3.75	6.31	8.39	3.98	3.20	2.84	5.04d
45	5.77	3.42	6.28	3.29	3.90	1.93	1.89	3.78e
67	3.93	3.56	5.30	1.53	3.77	1.91	3.23	3.32f
89	2.25	3.74	2.40	3.32	1.59	2.67	2.14	2.59g
112	1.67	1.48	1.60	4.63	2.28	1.84	3.00	2.36h
134	1.67	2.88	1.80	3.93	3.70	5.05	2.31	3.05
156	1.38	1.41	0.90	1.93	5.27	3.76	1.30	2.28i
178	0.66	0.12	3.30	1.57	4.27	3.20	2.24	2.19j
189	-	-	-	2.94	3.28	1.47	2.11	2.45k
Total	49.40	36.29	49.10	46.80	50.60	35.30	31.10	-
Mean ^{&}	4.49	3.30	4.46a	3.90b	4.22c	2.94d	2.59e	3.70
S.D.	3.30	1.94	2.52	2.00	1.61	1.13	0.72	1.40
CV	73.5	58.8	56.5	51.3	38.2	38.4	27.8	37.8

* column samples with decreasing trend in macroporosity with depth at 5% level of significance ($P < 0.05$) based on the Kendall test for trends

^{NS} column samples with no significant trend in macroporosity with depth

[&] mean macroporosity estimated from samples at the different depths (column) and for different samples (row). Values with different letter in the same column (for depth) or rows (for samples) are significantly different ($p < 0.05$).

the column, where the macroporosity was estimated at 15.76%. This result was found from the image analysis to be a burrow, possibly created by ants or termites. On further analysis of the slices from that section, it was found that the burrow occupied one half of the section at that depth, with estimated macroporosity values of 24.60 and 23.80% at the top and bottom quadrants of this section. The presence of such larger than average cavities in natural soils is not unusual, especially in no-till fields like the test plot. Such a phenomenon in natural soils supports the use of undisturbed soil columns for macropore studies.

The above data regarding total macroporosity clearly indicate the existence of more macropores with diameters 0.54 mm or greater in the A-horizon than in the B-horizon. The data also indicate a greater decrease in soil macroporosity with depth in the A-horizon than in the B-horizon. As shown in Fig. 4, the top 50 mm depth of the A-horizon had an average macroporosity of 5.09%, which decreased to an average value of 2.60% in the rest of the A-horizon. This was a decrease of

48.9%. However, the macroporosity in the B-horizon in the top 50 mm had an average value of 2.39%, which decreased to 1.63% in the rest of the horizon. These results indicate that most of the macropores in this soil were prevalent in the top 50 mm depth, decreasing along the soil profile into the B-horizon. These results were further supported by observations of earthworms (*Lumbricus terrestris* L). The work of this species of earthworm has been observed to alter the top horizon of forest soils by their habit of pulling leaf litter into their burrows up to depths of about 100 mm (Hole 1981).

The results have also been compared to those from other studies involving physical counting of macropores (Ehlers 1975; Shipitalo et al. 1990; Phillips et al. 1995) and using image analysis on thin impregnated sections from different depths (Moran et al. 1988; Bullock and Thomasson 1979). Ehlers (1975) investigated macropores created by earthworms for tilled and untilled fields at different depths by counting the pores at different depths in the field. The study concluded that the volume percentage occupied by channels (macroporosity) was rather low (less than one volume percent) even in the B₁ horizon, which had the highest density of channels in both tilled and untilled plots. A similar low macroporosity value of 0.58% for pores with effective diameters of 2 mm or larger was mapped under a no-till soil block measuring 300 x 300 x 300 mm (Shipitalo et al. 1990). These comparatively low values may be the result of not being able to identify pores with diameters less than 1.0 mm with the naked eye. Secondly, these values represent the macroporosity of just one particular depth and, in fact, compare rather well with values at individual depths in the present study. Using a tension infiltrometer, Watson and Luxmoore (1986) estimated the mean macroporosity (pores \leq 1.0 mm) of 30 samples to be 0.04% in a forest watershed soil. Besides using bigger diameter macropores, the ponded- and tension-infiltrometer procedure determines the hydrologically-active macroporosity without accounting for macropores that are blocked or are not conducting for other reasons.

Although the effective diameters, soil characteristics, and management practices were different in the various studies mentioned above, the range of macroporosity obtained through the A and B horizons in the present study compares well with the range reported in the above studies. These results also provide strong evidence that macroporosity values obtained at just one or two depths in a soil profile may provide a very poor or erroneous representation of macroporosity throughout the horizon.

Table IV. Soil macroporosity distribution with depth in the B-horizon of a no-till silt loam soil from Belmont, ON estimated from CT scanning.

Depth (mm)	Total Macroporosity (%) - B-horizon								Mean ^{&}
	S1 ^{NS}	S2 ^{NS}	S3 ^{NS}	S4 ^{NS}	S5 ^{NS}	S6 [*]	S7 ^{NS}	S8 ^{NS}	
0	0.93	2.34	3.69	1.37	3.62	2.99	1.18	1.26	2.17a
12	0.56	1.18	1.92	2.28	2.73	15.8	0.83	0.80	3.26
23	2.07	1.48	4.31	3.17	3.86	4.89	1.28	0.73	2.72b
34	0.71	1.44	2.94	1.24	2.98	4.83	1.01	0.49	1.96c
45	0.66	1.39	1.56	1.96	2.76	4.06	1.54	0.62	1.82d
67	0.63	0.81	1.14	0.50	1.25	3.23	1.02	0.57	1.14e
89	0.89	0.64	1.37	1.10	1.10	3.32	0.82	1.06	1.29f
112	1.25	0.84	3.41	1.74	0.97	1.49	0.69	0.35	1.34g
134	1.84	1.60	3.09	1.65	1.56	2.12	0.98	2.62	1.93
156	1.98	0.77	1.34	0.89	5.33	1.87	1.68	1.06	1.87
178	2.29	1.10	3.16	1.89	3.50	1.17	2.23	1.10	2.06
189	-	0.97	-	1.40	1.47	1.78	3.23	-	1.77
Total	13.88	14.56	27.90	19.20	31.10	47.5	16.5	10.70	-
Mean	1.26a	1.21b	2.54c	1.60d	2.59e	3.96f	1.37g	0.97h	1.94
S.D.	0.66	0.47	1.10	0.70	1.35	3.93	0.73	0.62	0.59
CV	0.524	0.388	0.433	0.438	0.511	0.992	0.533	0.639	0.304

* column samples with decreasing trend in macroporosity with depth at 5% level of significance ($P < 0.05$) based on the Kendal test for trends

^{NS} column samples with no significant trend in macroporosity with depth

[&] mean macroporosity estimated from samples at the different depths (column) and for different samples (row). Values with different letter in the same column (for depth) or rows (for samples) are significantly different at ($p < 0.05$).

Bullock and Thomasson (1979) used image analysis to investigate the macroporosity (defined for effective diameters of 0.06 mm and greater) of six agricultural soils with different soil structure and management practices at four different depths up to about 1000 mm. These depths included the A and B horizons and in a couple of the samples part of the C horizon. In all six soils, the A-horizon up to about 180 mm had an average macroporosity of 6.80% and the B-horizon up to a depth of about 450 mm had an average macroporosity of 8.53%. The higher B-horizon value was explained to be the result of previous management in most of the soils affecting macropores in the top soil. Three of the soils had B-horizon values which measured two to three times the corresponding A-horizon values.

The relative contribution of macroporosity to total porosity reveals that soil macropores constituted a very small fraction (less than 10 percent) of the total porosity of the soil profiles studied (Fig 6). The A-horizons had an average of 7.76% of the

total porosity being contributed by macroporosity (pores ≥ 0.54 mm), with values ranging from 10.10% in S1 to 5.32% in S8. The B horizons had a somewhat lower average value of 4.92% with values ranging from 10.19% in S6 to 2.42% in S8. These results imply that, on average, the remaining 92.24 and 95.84% of the total porosity of the A and B horizons, respectively, are due to voids with effective diameters less than 0.54 mm or what may be referred to as the micropore component.

The relative contribution of micropores and macropores to the total porosity for each column also indicates more activities by macropore-forming organisms, namely earthworms, termites, ants, plant roots, and branches, in the A-horizon than in the B-horizon. Factors that may contribute to this include reduced tillage and the availability of plant residue and mulch close to the surface. The reduced tillage conditions and the presence of adequate supply of surface mulch cause the soil to be wetter and cooler during the summer months, creating a more favourable environment for the large surface-feeding earthworms (Ehlers 1975; Omoti and Wild 1979). The absence of tillage also provides a safe zone close to the surface for these organisms, and allows the earthworm burrows to persist and potentially become preferential pathways for water and solute.

Investigating trends in macroporosity with depth

One important aspect of the characterization of the soil macropores was an analysis of trends in the soil macroporosity with depth. There has been a general belief that soil macroporosity reduces with depth from the soil surface (Edwards et al. 1988; Omoti and Wild 1979). Ehlers (1975) reported that the number of earthworm channels increased with depth down to 60 mm in both tilled and untilled soil. An investigation in this study in relation to trends explored whether soil macroporosity values significantly decreased with depth; for these macroporosity values obtained at different depths, did they relate to each other in a monotonic fashion, and if so, in how strong a relationship. This investigation was aimed separately at the A and B horizons, covering 0 - 200 mm and 200 - 400 mm depths, respectively, and also on the whole soil profile from 0 - 400 mm depth. The Kendall test for trends

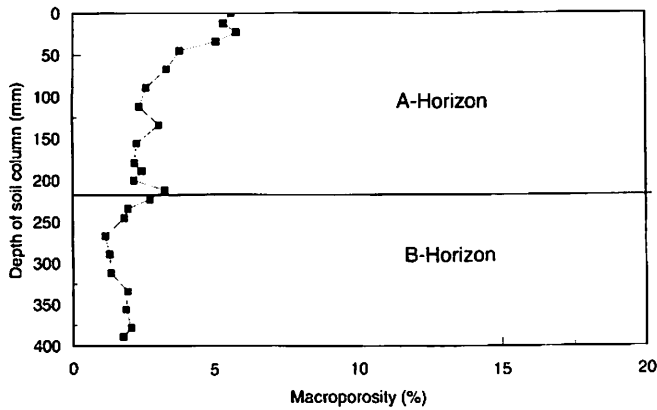


Fig. 4. Estimated macroporosity (pores > 0.54 mm) at different depths for the A and B horizons of the Tavistock silt loam (each value is the average obtained from seven and eight column samples for the A and B horizons, respectively).

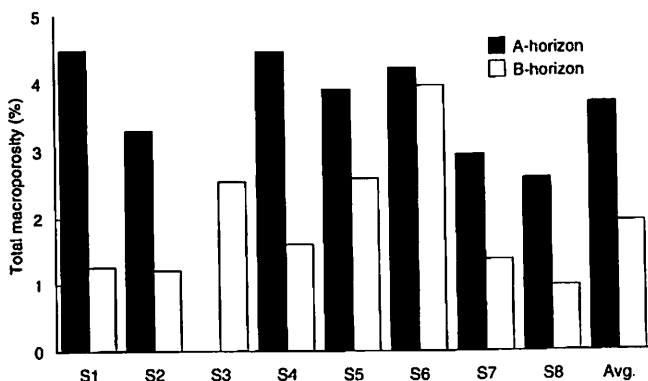


Fig. 5. Total macroporosity (pores > 0.54 mm) of the A and B horizon columns (values are the averages for the 11 depths).

(McCuen 1992), intended to assess the randomness of a data sequence, was used in this case to assess whether the soil macroporosity values constituted a homogenous series. The Kendall non-parametric test has received comprehensive assessment in the literature (Hirsch et al. 1982, 1992; SYSTAT for Windows 1992). Hirsch et al. (1982) described this test as an effective and general measure of trends and because it is a rank-based procedure, it has been found to be resistant to the effect of extreme values and to deviations from a linear relationship. This property makes it very suitable for testing the macroporosity with depth data such as that in Tables III and IV, which clearly indicate the presence of extreme high and low values, and an obvious absence of a linear relationship.

The Kendall test is based on a null hypothesis that the data constitute a sample of n independent and identically distributed random variables (i.e. a homogenous series) and on an alternative hypothesis that the distributions are not identical. The test is designed to detect a monotonically increasing or decreasing trend in data rather than the occurrence of an episodic event. The theorem defining the test statistics has been well documented by McCuen (1992).

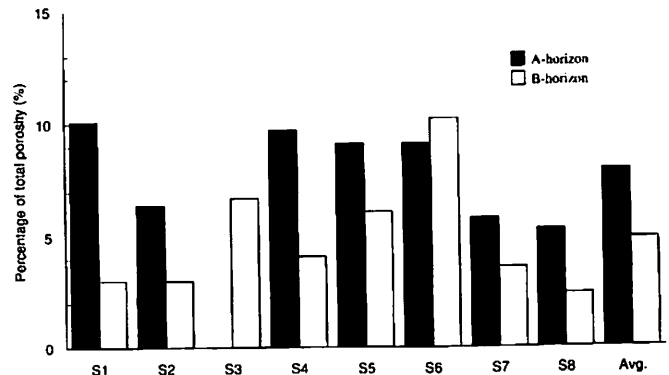


Fig. 6. Contribution of soil macroporosity (pores > 0.54 mm) to the total porosity of the soil.

Results from the A-horizon sample showed a marked decreasing trend in macroporosity with depth for samples S1A, S2A, S4A, and S5A at an error level of $P < 0.05$. The remaining three samples S6A, S7A, and S8A did not show any significant trend, neither increasing or decreasing, in the macroporosity values with depth. The mean values for all the samples in the A-horizon showed a decreasing trend in the macroporosity with depth at the same level of significance.

All the B-horizon samples showed absolutely no significant trend, either decreasing or increasing, in the macroporosity values with depth, including the means, with the exception of Sample S6B which showed a decreasing trend. When the test was conducted on the two profiles together (0 - 400 mm depth), the results indicated a significant decreasing trend in macroporosity with depth in all the samples as well as the means.

Relating macroporosity to physical properties of soil

Results from the principal component analysis (PCA) using the A horizon data revealed that bulk density and saturated hydraulic conductivity were correlated with macroporosity, with coefficients of 0.621 and -0.567, respectively. These correlation coefficients indicate that each of correlated variables, considered alone, explained 38.6% and 32.1% of the variability in the total macroporosity. Only the bulk density was considered in the PCA because the two variables appeared in the same significant principal component. The correlations for silt and clay content were quite low as indicated in Table V. For the A horizon data, the predictor variables selected for macroporosity based on the number of significant principal component using Kaiser's rule and the communalities (McCuen 1992) were bulk density, water content, and percentage silt and clay contents.

In the B-horizon data, only saturated hydraulic conductivity had a significant linear association with total macroporosity with a correlation coefficient of 0.723, indicating saturated hydraulic conductivity accorded 52.3% of the variability to in macroporosity (Table V). Thus bulk density, saturated hydraulic conductivity, and water content were selected as predictor variables forming significant principal components.

Multiple regression relations were developed using the total macroporosity in the A and B horizons as criteria variables; Bulk density, water content, and percent silt and clay content were utilized as the predictor variables for the A horizon and

Table V. Correlation coefficients of total macroporosity.

Soil physical properties	A-Horizon	B-Horizon
Sand	-0.018	-0.002
Silt	-0.158	0.229
Clay	0.086	-0.148
Water content	0.404	-0.239
Bulk density	0.621*	0.072
Hydraulic conductivity	0.567*	0.723*

* Correlation with macroporosity was significant at the 95% probability level.

Table VI. Coefficients from multiple regressions derived with Eqs. 2a and 2b.

Soil physical properties	Regression Coefficients
A Horizon	
Constant	$A_0 = 4.976$
Bulk density (β_b)	$A_1 = 13.920$
Volumetric water content (θ_v)	$A_2 = 31.991$
Silt	$A_3 = -0.550$
Clay	$A_4 = -0.119$
Coefficient of determination (R^2)	0.883
Standard error of estimate (SEE)	0.431
B Horizon	
Constant	$B_0 = -12.960$
Saturated hydraulic conductivity (K_s)	$B_1 = 13.920$
Bulk density (β_b)	$B_2 = 13.920$
Volumetric water content (θ_v)	$B_3 = 31.990$
Coefficient of determination (R^2)	0.619
Standard error of estimate (SEE)	0.830

saturated hydraulic conductivity, bulk density, and water content utilized for the B horizon. The objective was to try and improve the prediction accuracy and the ability to measure the effect of each predictor on total macroporosity. Following McCuen (1992), the relationship developed was of the form:

$$F_A = A_0 + A_1 \rho_b + A_2 \theta_v + A_3 \text{ silt} + A_4 \text{ clay} \quad (2a)$$

$$F_B = B_0 + B_1 K_s + B_2 \rho_b + B_3 \theta_v \quad (2b)$$

where:

F_A, F_B = total macroporosity for the A and B horizons(%),
 ρ_b = bulk density (kg/m^3),
 θ_v = volumetric water content (m^3/m^3),
 K_s = saturated hydraulic conductivity (m/s^1),
silt = silt content (%),
clay = clay content (%),
 A_0, B_0 = constants,
 $A_1 \dots A_4$ = regression coefficient corresponding to each of the four predictor variables for A horizon, and
 $B_1 \dots B_3$ = regression coefficient corresponding to each of the three predictor variables for B horizon.

The multiple regression coefficients corresponding to bulk density, water content, silt content, and clay content for the A horizon and the saturated hydraulic conductivity, bulk density, and water content for the B horizon macroporosity are presented in Table VI. Their corresponding coefficient of multiple determination (R^2) and standard errors of estimates (SEE) are also presented in Table VI.

The multiple regression relationships predicted the observed macroporosity data in the A and B horizons with R^2 values of 0.883 and 0.619, respectively. These results indicate that each equation explained the variations in total macroporosity to a different extent in the A horizon (88%), B horizon (62%). This, in addition to the differences in the regression coefficients, reflects the impact of the variability of the soil properties on the soil macroporosity. The standard error of estimates for the four-predictor model of the A-horizon macroporosity was 0.431, and for the three-predictor model of the B-horizon macroporosity was 0.830. Still the values were high and the goodness-of-fit statistics indicate that the multiple regression model will provide somewhat marginally accurate estimates of the total macroporosity values.

CONCLUSIONS

This study reveals that the volume CT scanner provides a non-destructive technique to estimate macroporosity in soil columns. This study also provides evidence that, at least for silt loam soil managed for several years in no-till conditions:

1. The total macroporosity in the A and B horizons is likely to be very small (in the order of 4 and 2%, respectively), and is likely to be lower in the B-horizon with significantly lower variability with depth than in the A-horizon.
2. The relative contributions of macroporosity to the total porosity in the A and B horizons are in the order of 8 and 5%, respectively.
3. There is likely to be a significant decreasing trend of macroporosity with depth through the A-horizon and through the combined A and B horizons, but not necessarily through the B horizon itself.
4. Bulk density and saturated hydraulic conductivity are highly correlated with the total macroporosity in the A horizon but only hydraulic conductivity correlates highly with the total macroporosity in the B horizon.

For the study site, there was also evidence of increased soil macropore formation activities in the A-horizon due to the

presence of earthworms. The bulk density, total porosity, and organic matter content of silt loam soil were found to be significantly different in the A and the B horizons.

ACKNOWLEDGMENT

The research was supported financially through grants provided by the Natural Science and Engineering Research Council of Canada (NSERC). Research facilities were also made available by the Agricultural and Agri-Food Canada, London and Guelph, ON; and the Robarts Research Institute, London, ON.

REFERENCES

- Agricultural Canada. 1990. *Soil Survey of the Pilot Watersheds Southwestern Ontario Soil and Water Environmental Enhancement Program, (GAG05)*. Ottawa, ON: Department of Supply and Services, Agriculture Canada.
- Anderson, S.H., C.J. Gantzer, J.M. Boone and R.J. Tully. 1988. Rapid nondestructive bulk density and soil-water content determination by computed tomography. *Soil Science Society American Journal* 52:35-40.
- Anderson, S.H., R.L. Peyton and C.J. Gantzer. 1990. Evaluation of constructed and natural soil macropores using x-ray computed tomography. *Geoderma* 46:13-29.
- Andreini, M.S. and T.S. Steenhuis. 1990. Preferential paths of flow under conventional and conservation tillage. *Geoderma* 46:85-102.
- Bouma, J. 1981. Measuring the hydraulic conductivity of soil horizons with continuous macropores. *Soil Science Society American Journal* 46:438-441.
- Bullock, P. and A.J. Thomasson. 1979. Rothamsted studies of soil structure, 2, Measurements and characterization of macroporosity by image analysis and comparison with data from water retention measurements. *Journal of Soil Science* 30:391-414.
- Edwards, W.M., L.D. Norton and C.E. Redmond. 1988. Characterizing macropores that affect infiltration into nontilled soils. *Soil Science Society of America Journal* 52:483-487.
- Edwards, W.M., M.J. Shipitalo, L.B. Owens and L.D. Norton. 1990. Effect of *Lumbriscus Terrestris* L. burrows on hydrology of continuous no-till corn fields. *Geoderma* 46:73-84.
- Ehlers, W. 1975. Observations on earthworm channels and infiltration on tilled and untilled loess soil. *Soil Science* 119(3):242-249.
- Gardner, W.H. 1962. How water moves in the soil. *Crops Soils* 15(10):7-11.
- Gish, T.J., C.S. Helling and M. Mojasevic. 1991. Preferential movement of atrazine and cyanazine under field conditions. *Transaction ASAE* 34(4):1699-1705.
- Hirsch, R.M., D.R. Helsel, T.A. Cohn and E.J. Gilroy. 1992. Statistical analysis of hydrologic data. In *Handbook of Hydrology*, ed. D. R. Maidment. 17.1-17.55. New York, NY: McGraw-Hill Inc.
- Hirsch, R.M., J.R. Slack and R.A. Smith. 1982. Techniques of trend analysis for monthly water quality data. *Water Resources Research* 18:(1)107-121.
- Holdsworth, D.W., M. Drangova and A. Fenster. 1993. A high resolution XRIT-based quantitative volume CT scanner. *Medical Physics* 20(2):449-462.
- Hole, F.D. 1981. Effects of animals on soil. *Geoderma* 25:75-112.
- Joschko, M., O. Graff, P.C. Muller, K. Kotzke, P. Linder, D.P. Pretschner and O. Larink. 1991. A non-destructive method for the morphological assessment of earthworm burrow systems in three dimensions by X-ray computed tomography. *Biology and Fertility of Soils* 11:88-92.
- Li, Y. and M. Ghodrati. 1994. Preferential transport of nitrate through soil columns containing root channels. *Soil Science Society American Journal* 58:653-659.
- McCuen. 1992. *Microcomputer Applications in Statistical Hydrology*. Englewoods Cliffs, NJ: PTR Prentice Hall.
- McKeague, J.A. 1978. *Manual on Soil Sampling and Methods of Analysis*. Ottawa, ON: Canada Soil Survey Committee, Canadian Society of Soil Science.
- McMahon, M.A. and G.W. Thomas. 1974. Chloride and tritiated water flow in disturbed and undisturbed soil cores. *Soil Science Society of America Proceedings* 38:727-732.
- Moran, C. J., A.J. Koppi, B.W. Murphy and A.B. McBratney. 1988. Comparison of the macropore structure of a sandy loam surface soil horizon subjected to two tillage treatment. *Soil Use and Management* 4(3):96-101.
- Murphy, J.B., E.H. Grissinger and W.C. Little. 1981. Fiberglass encasement of large, undisturbed weakly cohesive soil samples. *Soil Science* 131(2): 130-134.
- Omoti, U. and A. Wild. 1979. Use of florescent dyes to mark the pathways of solution movement through soils under leaching conditions: 2. Field experiments. *Soil Science* 28(2): 98-104.
- PCI Software. 1994. EASI/PACE image analysis soft ware version 5.3, *Using PCI Software Vol. 1*. Richmond Hill, ON: PCI Inc.
- Petrovic, A.M., J.E. Siebert and P.E. Rieke. 1982. Soil bulk density analysis in three dimensions by computed tomographic scanning. *Soil Science Society American Journal* 46(3):445-450.
- Peyton, R.L., C.J. Gantzer, S.H. Anderson, B.A. Haeffner and P. Pfeifer. 1994. Fractal dimension to describe soil macropore structure using x-ray computed tomography. *Water Resources Research* 30(3):691-700.
- Peyton, R.L., B.A. Haeffner, S.H. Anderson and C.J. Gantzer. 1992. Applying x-ray CT to measure macropores diameters in undisturbed soil core. *Geoderma* 53:329-340.
- Phillips, R.E., V.L. Quisenberry and J.M. Zeleznik. 1995. Water and solute movement in an undisturbed, macroporous column: Extraction pressure effects. *Soil Science Society American Journal* 59:707-712.
- Quisenberry, V.L. and R.E. Phillips. 1978. Displacement of soil water by simulated rainfall. *Soil Science Society American Journal* 42:675-679.
- Quisenberry, V.L., R.E. Phillips and J.M. Zeleznik. 1994. Spatial distribution of water and chloride macropore flow in well- structured soil. *Soil Science Society American Journal* 58:1294-1300.

- Shipitalo, M.J., W.M. Edwards, W.A. Dick and L.B. Owens. 1990. Initial storm effects on macropore transport of surface-applied chemicals in no-till soil. *Soil Science Society American Journal* 54:1530-1536.
- Shipitalo, M.J. and R. Protz. 1987. Comparison of morphology and porosity of a soil under conventional and zero tillage. *Canadian Journal of Soil Science* 67:445-456.
- Singh, P. and R.S. Kanwar. 1991. Preferential solute transport through macropores in large undisturbed saturated soil columns. *Journal Environmental Quality* 20:295-300.
- Smettem, K.R.J. and N. Collis-George. 1985. Statistical characterization of soil peel method. *Geoderma* 36:27-36.
- Steenhuis, T.S., W. Staubitz, M.S. Andreini, J. Surface, T.L. Richards, R. Paulsen, N.B. Pickering, J.R. Hagerman and L. D. Geohring. 1990. Preferential movement of pesticides and tracers in agricultural soils. *Journal of Irrigation and Drainage Engineering* 116(1):50-66.
- SYSTAT for Windows. 1992. *Statistics, Version 5 Edition*. Evanston, Ill: SYSTAT, Inc.
- Warner, G.S., J.L. Nieber, I.D. Moore and R.A. Geise. 1989. Characterising macropores in soil by computed tomography. *Soil Science Society of America Journal* 53(3):653-660.
- Warner, G.S. and J.L. Nieber. 1991. Macropores distributions in tilled vs. grass-surfaced cores as determined by computed tomography. In *Proceedings of the National Symposium on Preferential Flow*, eds. T. J. Gish and A. Shirmohammadi, 173-182. St Joseph, MI, ASAE.
- Watson, K.W. and R.J. Luxmoore. 1986. Estimating macroporosity in a forest watershed by use of a tension infiltrometer. *Soil Science Society of America Journal* 50:578-582.
- Wildenschild, D., K.H. Jensen, K. Villholth and T.H. Illangasekare. 1994. A laboratory analysis of the effect of macropores on solute transport. *Ground Water* 32(3):381-389.